

The hot side of the lithium dip – LiBeB abundances beyond the main sequence

Corinne Charbonnel¹, Suzanne Talon^{2,3}

¹ Laboratoire d'Astrophysique de Toulouse, CNRS UMR5572, OMP, 14, Av. E.Belin, 31400 Toulouse, France

² Département de Physique, Université de Montréal, Montréal PQ H3C 3J7, Canada

³ CERCA, 5160 boul. Décarie, Montréal PQ H3X 2H9, Canada

Received 30 July 1999 / Accepted 13 September 1999

Abstract. We extend to the case of A and early-F type stars our study of the transport of matter and angular momentum by wind-driven meridional circulation and shear turbulence. We show that our fully consistent treatment of the same hydrodynamical processes which can account for C and N anomalies in B type stars (Talon et al. 1997) and for the shape of the hot side of the Li dip in the open clusters (Talon & Charbonnel 1998) also explains LiBeB observations in stars with T_{eff} higher than 7000 K on the main sequence as well as in their evolved counterparts.

Key words: Li dip; hydrodynamics; turbulence; Stars: interiors, rotation, abundances

1. Lithium abundance on the hot side of the dip

Due to its fragility to nuclear reactions, lithium is a very powerful tracer of the physical conditions in stellar interiors. During the last two decades, numerous abundance determinations of Li for both field and cluster low mass stars have indeed brought to light the occurrence of transport processes of chemicals in stellar radiative zones.

One of the most striking signatures of this (these) mechanism(s) is the drop-off in the lithium content of main sequence F-stars in a range of 300 K in effective temperature centered around 6700 K, first discovered in the Hyades by Wallerstein et al. (1965) and later confirmed by Boesgaard & Tripicco (1986). This feature appears in all galactic clusters older than ~ 200 Myrs as well as in field stars (see Michaud & Charbonneau 1991 and Balachandran 1995 for references).

Relatively few abundance determinations are available for main sequence cluster stars on the hot side of this so-called lithium dip. The scarceness of data is due to the fact

Send offprint requests to: Corinne Charbonnel ; corinne@obs-mip.fr

that lithium can be observed in slow rotators only ($V \sin i$ lower than ~ 70 km.sec⁻¹), while most of the stars on the hot side of the dip are actually fast rotators. In the Hyades, Praesepe and Coma¹, these objects show lithium abundances close to the galactic value ($\log N(\text{Li}) \simeq 3.31$, with $\log N(\text{H}) = 12$), except for a few Li deficient Am-stars (Boesgaard 1987, Burkhardt & Coupry 1989, 1998², 1999). In the field, the occurrence of Li-underabundant main sequence (or slightly evolved) stars originating from the hot side of the dip is not rare (Balachandran 1990, Burkhardt & Coupry 1991). For these objects, the lithium abundance shows indeed a dispersion of one order of magnitude below the galactic value.

Among the different processes which have been proposed to account for the lithium distribution in Pop I low-mass stars³, atomic diffusion is the only one which can be calculated from first principles without any arbitrary parameter. Its importance has been spectacularly demonstrated in the Sun, thanks to helioseismology (Bahcall & Pinsonneault 1995, Christensen-Dalsgaard et al. 1996, Richard et al. 1996). The nature and strength of the abundance anomalies (for lithium, but also for helium and metals) due to diffusion alone are expected to change in the domain going from G to F and A stars due to the shallowing of the superficial H-He convective zone

¹ which all have approximately 700 Myrs

² In Praesepe, Am stars present the same Li abundance as F stars on the hot side of the lithium dip.

³ Gravitational settling and radiative diffusion (Michaud 1986, Proffitt & Michaud 1991, Richer & Michaud 1993), mass loss (Hobbs et al. 1989, Guzik et al. 1987, Schramm et al. 1990, Swenson & Faulkner 1992), meridional circulation (Charbonneau & Michaud 1988, 1990, 1991), turbulent mixing induced by rotation (Vauclair et al. 1978, Vauclair 1988, Pinsonneault et al. 1989, 1990, Deliyannis & Pinsonneault 1990, Charbonneau & Michaud 1991, Charbonnel et al. 1992, 1994, Charbonnel & Vauclair 1992, Chaboyer et al. 1995, Talon & Charbonnel 1998), gravity waves (Garcia Lopez & Spruit 1991, Montalbán & Schatzman 1994).

when T_{eff} increases and to the competition between radiative acceleration and gravitational settling. It has however been known for a long time (Michaud 1970, Michaud et al. 1976, Vauclair et al. 1978) that diffusion theory actually predicts abundance anomalies much larger than the ones observed, revealing the occurrence of some perturbing macroscopic process(es). New calculations performed by the Montreal group taking into account turbulent diffusion yield results in better agreement with observations, once more illustrating the need for an improved treatment of hydrodynamical processes (Richer et al. 1999a).

Regarding the F stars in the Li-dip region, carbon, oxygen and boron under-abundances are indeed expected in the case of pure diffusion (Michaud 1986, Turcotte et al. 1998), but are not observed in the Hyades members (Boesgaard 1989, Friel & Boesgaard 1990, Garcia Lopez et al. 1993) nor in the Be-deficient field stars (Boesgaard et al. 1977). In addition, in this framework Li settles and remains in a buffer zone below the convective envelope and should be dredged-up after the turnoff; this is not observed in M67 subgiant stars which originate from the dip (Pilachowski et al. 1988, Balachandran 1995, Deliyannis et al. 1997). This implies that another process competes with diffusion and leads to nuclear destruction of lithium inside the dip. Finally, a macroscopic process is expected to limit both the predicted Li overabundances due to radiative acceleration in stars with $T_{\text{eff}} \simeq 7000$ K (Michaud 1986), and the predicted strong Li underabundances due to settling for stars with $T_{\text{eff}} > 7200$ K (Richer & Michaud 1993), which are not observed in open clusters. The overabundance problem is less crucial compared to previous studies with the new radiative force calculations by Richer et al. (1999b), who follow the strong coupling that exists between the atomic diffusion of one element and the abundance of another one (Richer et al. 1997). Indeed, in these stars the radiative acceleration on lithium is never higher than gravity, but of the same order of magnitude. However, the behavior of the more massive stars remains puzzling.

Important clues for understanding the macroscopic processes that compete with atomic diffusion in A and F stars come from lithium observations in subgiant stars originating from the hot side of the dip. Looking at subgiants rather than giants allows to track signatures of mechanisms acting deep in the star on the main sequence while permitting to avoid further complications due to possible lithium destruction in more advanced stages (see Charbonnel 1995). Observations by Alschuler (1975) of a few field stars crossing for the first time the Hertzsprung gap indicated that lithium depletion starts earlier than predicted by standard dilution for stars more massive than $2 M_{\odot}$. Later on, significant lithium depletion was observed in a non negligible number of slightly evolved field stars (Brown et al. 1989, Balachandran 1990). Recently, Dias et al. (1999) studied the behavior of lithium in an homogeneous sample of field subgiants observed by Lèbre et al.

(1999) for which Hipparcos data allowed the precise determination of both the evolutionary status and the mass. They confirmed that stars originating from the hot side of the dip present a large range of lithium abundances which can not be explained by standard dilution alone and which reflect different degrees of depletion of this element while on the main sequence, even if its signature does not appear at the stellar surface at the age of the Hyades (see Vauclair 1991, Charbonnel & Vauclair 1992). In this cluster, dilution is not sufficient to explain lithium values in evolved stars (which have masses of the order of $2.2 M_{\odot}$), while main sequence stars present galactic abundance (Boesgaard et al. 1977, Duncan et al. 1998). This has been observed also in open clusters with turnoff masses higher than $\sim 1.6 M_{\odot}$ (Gilroy 1989).

In Talon & Charbonnel (1998, hereafter TC98), we assessed the role of the wind-driven meridional circulation and of shear turbulence as described by Zahn (1992) and Maeder (1995) in the transport of chemicals and angular momentum in low mass stars. We showed that the shape of the hot side of the Li dip in the Hyades was successfully explained within this framework which also reproduces the C and N anomalies in B-type stars (Talon et al. 1997).

In the present paper we study the impact of rotational mixing in stars hotter than 7000 K, and extend our computations up to the completion of the first dredge-up in order to confront our predictions with observations in subgiant and giant stars. In §2 we recall the input physics of our models as well as the observational constraints on the evolution of the surface velocity. The global characteristics of the models are discussed in §3. We then present the theoretical predictions for the evolution of the LiBeB and helium abundances, and compare our results with observations for both field and cluster evolved stars in §4.

2. Models including rotational mixing and atomic diffusion

2.1. The transport processes

Our models (computed with the Toulouse-Geneva evolutionary code) include both element segregation and rotation-induced mixing, and we treat simultaneously the transport of matter and angular momentum. The internal rotation profile evolves self-consistently under the action of meridional circulation, which is treated as a truly advective process, as described by Zahn (1992) and of shear stresses, treated as a turbulent viscosity (cf. Talon & Zahn 1997). As mentioned in TC98, each of these two processes involves a free parameter of order unity. Here, we did not calibrate the parameters and simply used the values which had been used in previous calculations (TC98) namely $C_h = 1$ and $\nu_{\text{th}} = 2/5$. We recall that the first free parameter describes the weakening effect of the horizontal turbulence on the vertical transport of chemical (cf. Zahn 1992 for details) and the second free parameter describes

the weakening of the restoring forces of the density stratification on the development of the vertical shear. The vertical turbulent viscosity ν_v is then

$$\nu_v = \nu_{\text{th}} K \left(\frac{r}{N} \frac{\partial \Omega}{\partial r} \right)^2, \quad (1)$$

where N is the Brunt-Väisälä frequency and K is the thermal diffusivity. We refer to TC98 (see also Talon et al. 1997) for more details.

We do treat the atomic diffusion of H, He, CNO, Ne and Mg. The diffusion coefficients are computed with Paquette et al. (1986) prescription, and we include the diffusion due to gravity and to the concentration and thermal gradients. The case of the LiBeB elements is peculiar, since on the hot side of the dip they are (partly) supported by radiative acceleration which is of the same order of magnitude as gravity (cf. Richer et al. 1999b). We thus decided to compute their evolution due to the macroscopic mixing only.

2.2. Constraints on the evolution of the surface rotation

The observational data indicate that, at the age of the Hyades, stars on the hot side of the dip have kept their initial rotation velocities (due to their very shallow convection envelope), while cooler stars have already been spun down by a magnetic torque. To take into account the large dispersion of the observed $V \sin i$ in the mass range we consider, we computed models with different initial velocities: 100 km.sec⁻¹, which corresponds to the mean velocity of the Hyades stars with $T_{\text{eff}} > 7000$ K, and 50 and 150 km.sec⁻¹ (see Gaigé 1993 and TC98). When the star leaves the main sequence, the evolution of its surface rotation velocity in our models is due only to the stellar expansion and momentum redistribution, i.e., we do not treat magnetic braking. This has no influence on the light element evolution on the subgiant branch since during this phase the surface depletion is largely dominated by dilution.

2.3. Input physics and stellar masses

The stellar models presented here include the same physics as in TC98. The radiative opacities from Iglesias & Rogers (1996) are complemented by the low-temperature opacities Alexander & Ferguson (1995). The thermonuclear reaction rates are from Caughlan & Fowler (1988).

We chose $z = 0.20$ as the initial metallicity of our models in order to compare our results to observations in Pop I stars in general⁴. The initial helium content is 0.28. The relative ratios for the heavy elements correspond to the mixture by Grevesse & Noels (1993), and the isotopic ratios are from Maeder (1983).

⁴ In TC98 the initial mixture was suited for precise comparison to the Hyades cluster.

We performed our computations for three stellar masses, namely 1.5, 1.85 and 2.2 M_{\odot} . At the age of the Hyades, the first one has an effective temperature at the edge of the Li-dip, while the last one corresponds to a slightly evolved star.

In these models, we assumed that no mass loss takes place. Indeed, the evolution of the rotation velocities of A and F stars indicates that the matter leaving the stars provides no (significant) torque to their surface. The small amount of mass lost at the surface thus leaves the star with its own angular momentum. Taking this into account in the numerical simulation would only marginally alter the result and we thus neglected it.

3. Global characteristics of the models

3.1. HR diagram

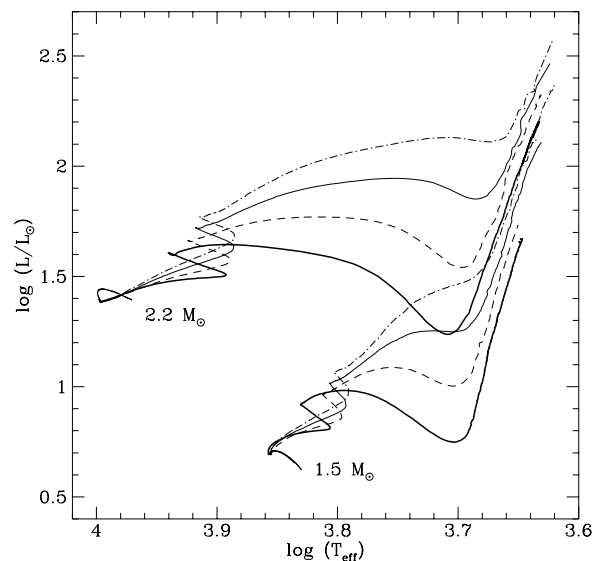


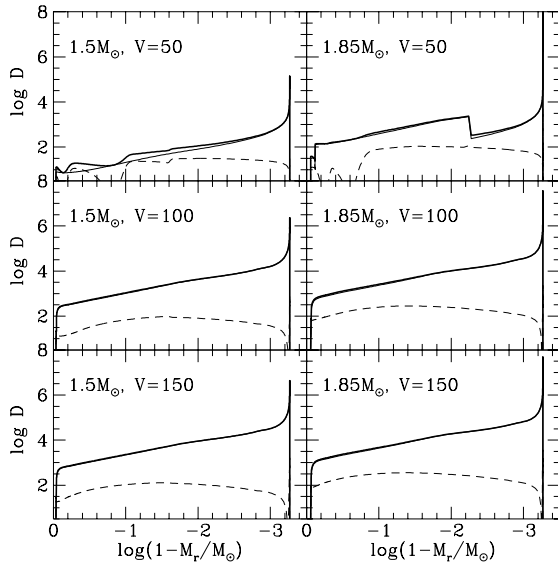
Fig. 1. Evolution of the models in the HRD from the zero age main sequence up to the completion of the first dredge-up (only two masses are shown for clarity). The solid, dashed and dashed-dotted lines correspond respectively to the stars with initial rotation velocities of 100, 50 and 150 km.sec⁻¹. The bold tracks are followed by non-rotating models

Fig. 1 displays the evolutionary paths followed by our models in the HR diagram⁵. In Table 1, we give their main

⁵ Let us notice that, on the scale of our HR diagram, the structural changes due to rotation are not visible on the ZAMS. Indeed, rotating models have lower luminosities and effective temperatures due to the reduction of gravity close to the equator by the centrifugal force, leading also to longer main sequence lifetimes. Here however, for the 1.5 M_{\odot} rotating at 150 km.sec⁻¹, the difference in effective temperature on the ZAMS

Table 1. Characteristics of the stellar models at the end of the main sequence

M_*/M_\odot	V ($\text{km}\cdot\text{sec}^{-1}$)	t (Gyrs)	$\log T_{\text{eff}}$	$\log L/L_\odot$
1.5	150	2.52	3.797	1.078
	100	2.39	3.802	1.026
	50	2.24	3.808	0.975
	0	2.18	3.818	0.961
1.85	150	1.30	3.846	1.46
	100	1.25	3.851	1.412
	50	1.17	3.860	1.355
	0	1.13	3.870	1.323
2.2	150	0.784	3.902	1.788
	100	0.744	3.905	1.737
	50	0.709	3.913	1.676
	0	0.691	3.917	1.633

**Fig. 2.** Diffusion coefficient profiles at the age of the Hyades for the 1.5 and $1.85 M_\odot$ models and for the three different velocities. The bold line represents the total diffusion coefficient, the thin full line shows the turbulent diffusion coefficient, and the dashed line, the effective diffusion coefficient related to the meridional circulation. In all cases, turbulence dominates the transport of the chemicals. After the main sequence, the abundance evolution is largely dominated by the dredge-up

characteristics at the end of the main sequence. Values for standard models (with no rotation) are also quoted.

The differences of global characteristic between the models including mixing and the standard models is striking. Indeed, as a consequence of mixing, the abundance profiles inside the star are modified compared to the stan-

in only 30 K while the lifetime is lengthened (due to structural effects only) by about 15 Myrs.

ard ones. In particular, the slight changes in the helium profile (see Fig. 3 and §3.3) affect the evolution. Furthermore, since mixing keeps adding fresh fuel to the core, the lifetime on the main sequence increases with the rotation rate. At the turnoff, the faster models are cooler and more luminous than the models with slow or no rotation. When the star leaves the main sequence, the differences in opacity between the models lead to evolution at higher luminosity on the subgiant branch for the faster rotators (see §3.3).

3.2. Transport coefficients inside the stars

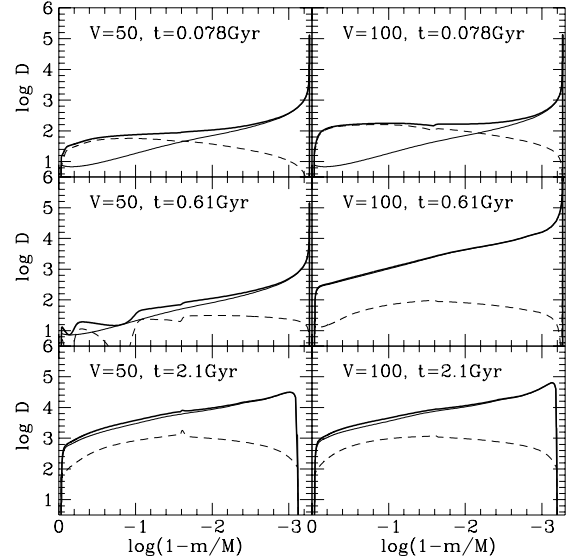
**Fig. 3.** Diffusion coefficient profiles at three ages the $1.5 M_\odot$ model for two different velocities. The line symbols are the same as in Fig 2

Fig. 2 shows the diffusion coefficients inside the models which are still on the main sequence at the age of the Hyades. In Fig. 3 we follow the evolution of these coefficients for the $1.5 M_\odot$ star with the lowest rotation velocities. During the first part of the evolution ($t = 78$ Myrs and also $t = 610$ Myrs for the slowest model), turbulence has not appeared yet and the full thin line represents only the lower limit of viscosity, namely radiative viscosity. Then settling of helium is possible, as can be seen in Figs. 5, 6 and 7. During that first period, meridional circulation advects momentum towards the interior, building up the differential rotation. When it becomes sufficient and for the rest of the main sequence evolution, turbulent diffusion dominates the transport of chemicals.

The situation is different for angular momentum though. Indeed, according to observations, main sequence stars hotter than the Li-dip are not slowed down by a

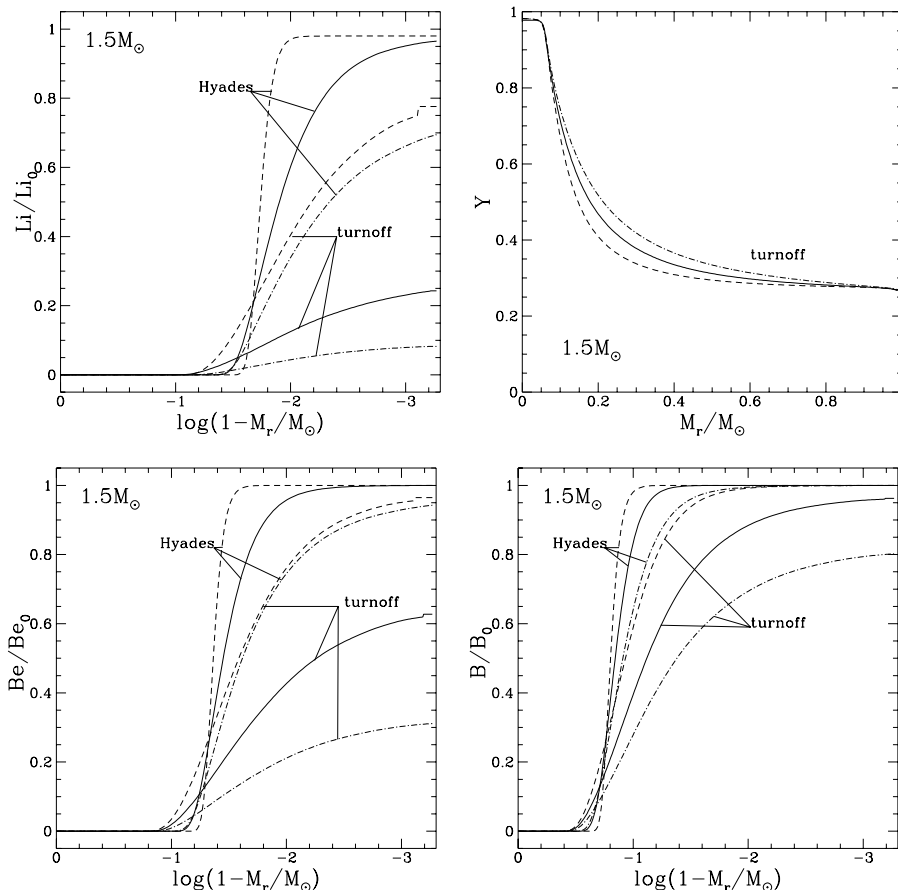


Fig. 4. Abundance profiles of LiBeB inside the $1.5 M_{\odot}$ star at the age of the Hyades and at the turnoff. The profiles of helium (in mass fraction) are shown at the turnoff only. The solid, dashed and dashed-dotted lines correspond respectively to the initial rotation velocities of 100, 50 and $150 \text{ km}\cdot\text{sec}^{-1}$

magnetic torque. As we discussed in TC98, since the complete equation for the transport of angular momentum admits a stationary solution, these stars soon reach a regime with no net angular momentum flux. The rotation profile results from the equilibrium of the advection of angular momentum by meridional circulation and of the turbulent diffusion due to shear turbulence⁶ which counterbalance each other. This stresses the need for a fully consistent treatment of the hydrodynamical processes present in stars.

3.3. Abundance profiles

In Fig. 4 we show the interior abundance profiles of the LiBeB elements in the $1.5 M_{\odot}$ model, at the age of the Hyades and at the turnoff for the three initial equatorial velocities. In the slowest model, the abundance profiles are relatively steep in the region of destruction of the LiBeB

elements by nuclear reactions. More rapid rotation leads to the destruction of these light elements in a larger region.

As can be seen on the profiles of helium (Fig. 4) and on the evolution of its surface abundance (Figs. 5, 6 and 7), the effect of microscopic diffusion is noticeable whatever the rotation velocity. The mixing tends to counteract it in the faster rotators, and leads to smaller variations of helium in the external regions. In the central regions, the mixing also affects the helium profile, leading to longer main sequence lifetime when the rotation rate is higher (see Table 1), and to slightly larger helium core mass. In addition, after the turnoff the deepening convective envelope of the faster rotators encounters a region with more helium than in slower models and thus, with a lower opacity. These stars consequently evolve at a higher luminosity on the subgiant branch.

4. Evolution of the surface abundances and comparison with observations

The evolution of the LiBeB and of the helium abundances at the stellar surface from the zero age main sequence

⁶ Remember we make the hypothesis that the major source of turbulence is shear.

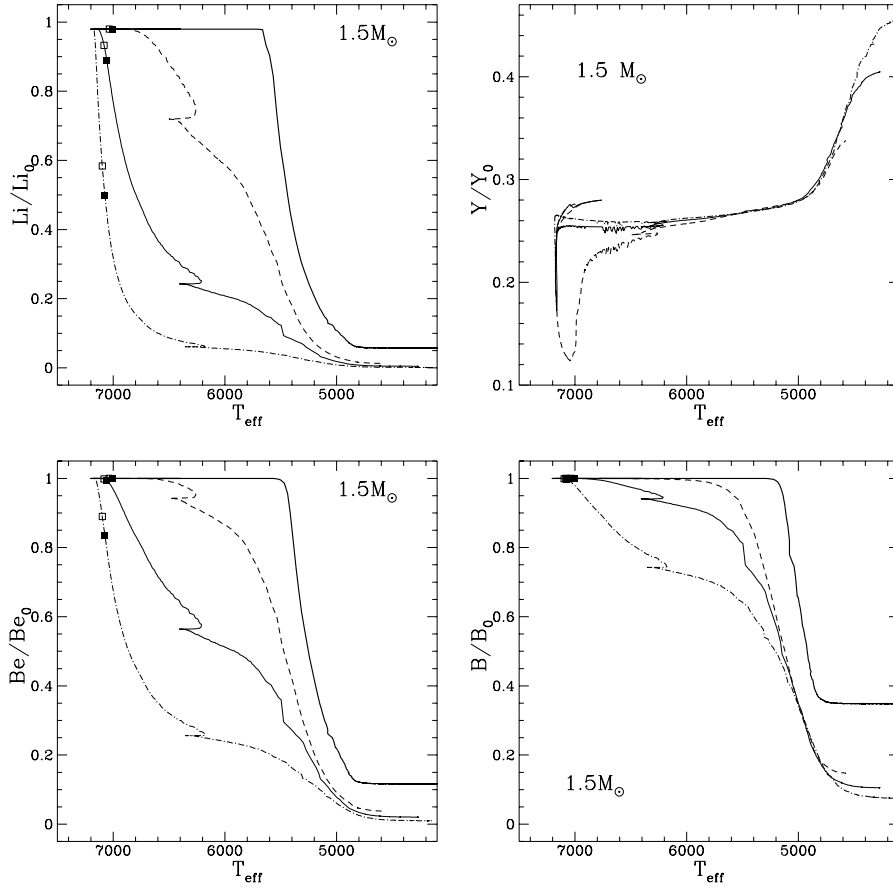


Fig. 5. Evolution of the LiBeB elements and of the helium mass fraction at the surface of the $1.5 M_{\odot}$ star as a function of its effective temperature. The line symbols are as in Fig. 1. The open and black squares indicate the evolutionary point at 0.7 and 0.8 Gyr respectively

up to the completion of the first dredge-up can be followed in Figs. 5, 6 and 7. We indicate the location of the stars at the age of the Hyades (since the main sequence lifetime of the models depends on their rotation rate, we quote both 0.7 and 0.8 Gyr). We also show the surface abundance variations for models computed without any transport process (no rotation mixing and no atomic diffusion), in order to locate the beginning of the standard first dredge-up. In the models with rotation, the change of slope around 5700-5800 K is a signature of this event.

4.1. Main sequence stars

Before discussing the LiBeB elements, one has to comment the evolution of the helium surface abundance. In all the rotating models, the effect of atomic diffusion is never completely cancelled. In the very early stages of main sequence evolution, helium settles (cf. Figs. 5, 6 and 7). Latter on, the increase of the macroscopic diffusion coefficients (cf. Fig. 3) leads to a partial dredge-up of helium. In the fast rotators ($V=100, 150 \text{ km}\cdot\text{sec}^{-1}$), this occurs very early on the main sequence, and the disappearance of the

He_{II} convection zone which is necessary to explain the Am phenomenon is not achieved. One may then find relatively few chemically peculiar stars with such a high rotation velocity, and the candidates would be very young objects. In the slow rotators ($V=50 \text{ km}\cdot\text{sec}^{-1}$) however, the helium dredge-up occurs later, and the stars can appear as chemically peculiar for most of their main sequence life. These predictions agree nicely with the observed velocity distribution of Am and normal A stars (Abt & Morrell 1995).

At the age of the Hyades, lithium, beryllium and boron are never depleted at the surface of the rotating main sequence stars on the hot side of the dip by more than about 70, 40 and 5% respectively. The larger depletion factors in the $1.85 M_{\odot}$ model compared to the $1.5 M_{\odot}$ one are due to the slightly larger diffusion coefficient and to the smaller convection envelope that empties more rapidly. More important LiBeB destruction is obtained in the $2.2 M_{\odot}$ model which is already evolved at the age of the Hyades.

Our predictions (obtained both in this paper and in TC98) are compared to the observations in the Hyades,

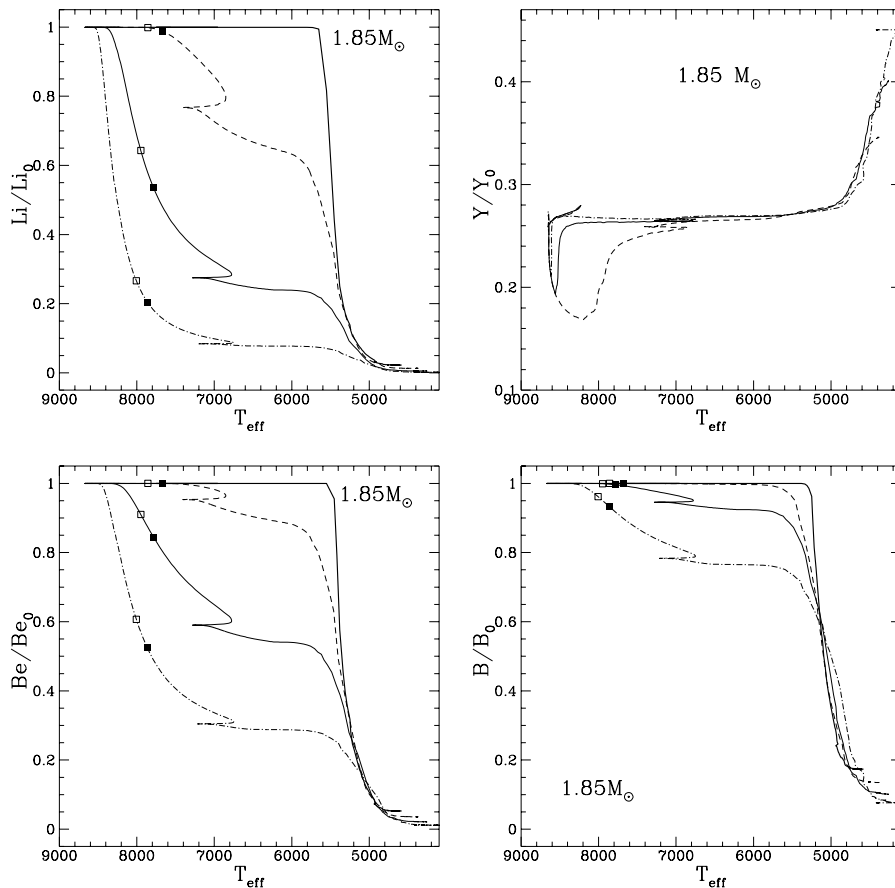


Fig. 6. Same as Fig. 5 for the $1.85 M_{\odot}$ star

Coma and Praesepe in Fig. 8. Let us recall that while the stars with $T_{\text{eff}} \leq 6900$ K lose angular momentum from their surface, the hotter ones conserve their global angular momentum during their main sequence life. In the domain we are interested in here, the weak differential rotation leads to diffusion coefficients that prevent any important surface lithium depletion at the age of the Hyades, in agreement with the observations.

The abundance of the LiBeB elements keeps decreasing while stars evolve. At the end of the main sequence, the maximum expected lithium depletion in the present models is of about one order of magnitude, in very good agreement with the observations in field main sequence stars originating from the hot side of the dip (Balachandran 1990, Burkhardt & Coupry 1991).

4.2. Evolved stars

Even if no important lithium depletion is expected at the surface of the main sequence stars on the hot side of the dip at the age of the Hyades, more lithium destruction occurs inside the rotating models compared to the standard case (see §3.3). This prepares the star to the lithium abundance variations observed in the latter evolutionary

phases. After the dredge-up, the LiBeB depletion is thus more important in the rotating models than in the models without transport processes (see Table 2), due to the enlargement of the LiBeB free regions.

The predicted evolution of the surface lithium abundance in our rotating models explains the behavior in the stars more massive than $1.5 M_{\odot}$ observed by Lèbre et al. (1999) and discussed by Dias et al. (1999). Indeed, for these objects a lithium dispersion of about two orders of magnitude is seen already at $T_{\text{eff}} \simeq 6300$ K, i.e. before the beginning of the standard dilution (at $T_{\text{eff}} \simeq 5600$ K). In the same homogeneous sample, the observed dilution factors are higher than the ones predicted by standard dilution alone. This is also seen in open cluster giants with turnoff masses higher than $1.5 M_{\odot}$ (Gilroy 1989) and in the large sample of field giants of Brown et al. (1989). As can be seen in Table 2, lithium depletion in giants down to factors as large as 1000 is well reproduced within our framework.

The effect is especially important for Li, which is the more fragile element. Regarding Be and B, the post-dilution values decrease at most by a factor of 3 (4) and 5 (11) respectively in the 2.2 (1.5) M_{\odot} model compared

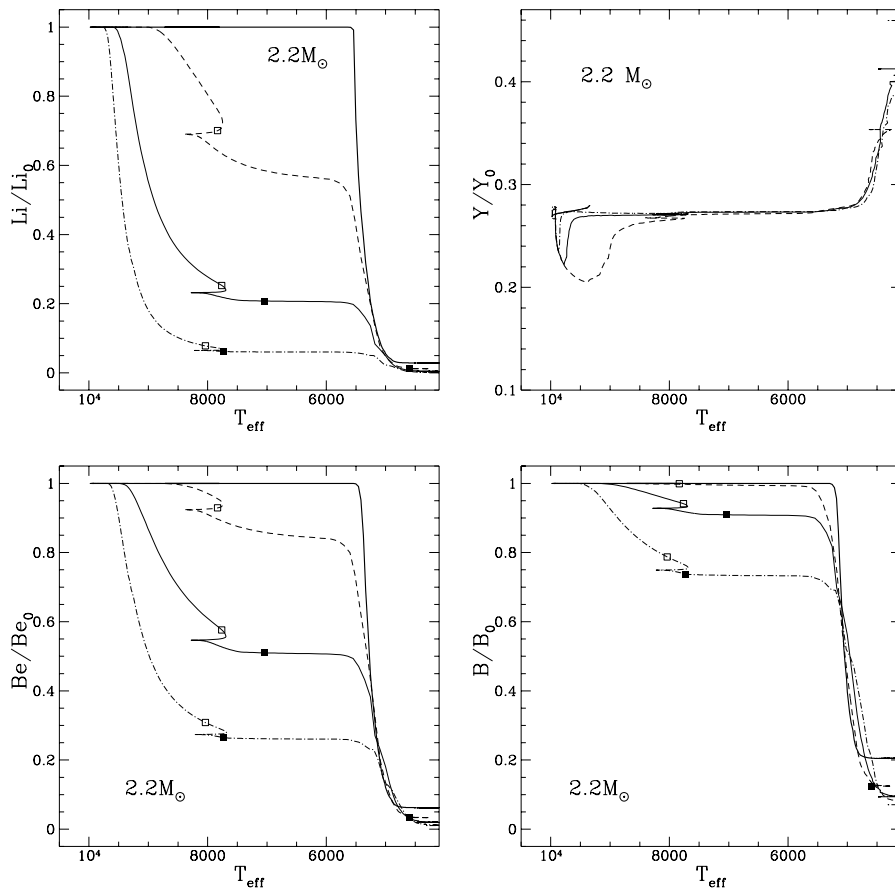


Fig. 7. Same as Fig. 5 for the $2.2 M_{\odot}$ star

to the case without mixing. From HST spectra, Duncan et al. (1998) determined a dilution factor of 1.0 ± 0.3 dex for B in two Hyades giants which present a lithium dilution factor of 2.2 ± 0.2 (see Table 2). These data are nicely explained by our rotating models.

5. Conclusions

In TC98, we presented stellar models including the most complete description currently available for rotation induced-mixing, taking into account simultaneously the transport of chemicals and the transport of angular momentum due to the wind-driven meridional circulation. We showed that the shape of the hot side of the Li dip in open clusters is well explained within this framework, which also successfully reproduces the C and N anomalies in B type stars (Talon et al. 1997).

In the present paper, we studied the impact of rotational mixing in A and early-F type stars on the main sequence and up to the completion of the first dredge-up. We showed that low lithium abundances measured in evolved stars originating from the hot side of the dip, which can not be explained by standard dilution alone, can be linked

simply to destruction in the interior of stars still on the main sequence. Such a destruction is not visible at the surface of the Hyades main sequence stars with $T_{\text{eff}} \geq 6900$ K simply because they are too young. More BeB data are needed to check the validity of our predictions for these elements.

Acknowledgements. We would like to thank Claude Burkhart for sending us data prior to publication. S.T. gratefully acknowledges support from FCAR of Quebec and NSERC of Canada.

References

- Abt H.A., Morrell N.I., 1995, ApJS 99, 135
- Alexander D.R., Fergusson J.W., 1994, ApJ 437, 879
- Alschuler W.R., 1975, ApJ 195, 649
- Bahcall J.N., Pinsonneault M.H., 1995, Rev.Mod.Phys. 67, 781
- Balachandran S., 1990, ApJ 354, 310
- Balachandran S., 1995, ApJ 446, 203
- Boesgaard A.M., 1987, PASP 99, 1067
- Boesgaard A.M., 1989, ApJ 336, 798
- Boesgaard A.M., Heacox W.D., Conti P.S., 1977, ApJ 214, 124
- Boesgaard A.M., Tripicco M.J., 1986, ApJ 302, L49
- Brown J.A., Sneden C., Lambert D.A., Dutchover E., 1989, ApJ Suppl 71, 293

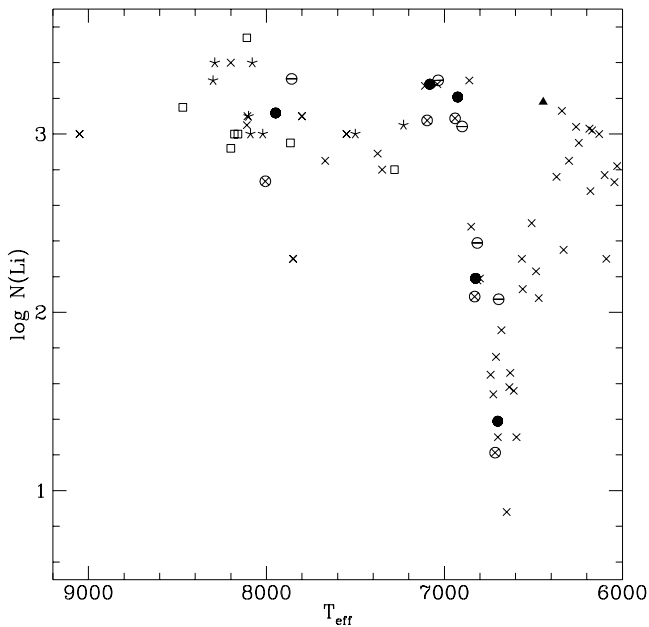


Fig. 8. Lithium abundance in the Hyades (crosses), Coma (squares) and Praesepe (asterisks; the lithium abundances for the Praesepe stars with $T_{\text{eff}} \simeq 8280$ K are upper values). The observations are from Boesgaard & Tripicco (1986), Thorburn et al. (1993), Burkhardt & Coupry (1998, 1999). Our predictions (present paper and TC98) are also shown for comparison (we use $\log N(\text{Li})_0 = 3.31$): The black dots correspond to calculations performed with an initial velocity of $100 \text{ km}\cdot\text{sec}^{-1}$, the pluses and minuses surrounded by a circle correspond to models with an initial velocity of 150 and $50 \text{ km}\cdot\text{sec}^{-1}$ respectively. The models with $T_{\text{eff}} \geq 6900$ K conserve global angular momentum during their main sequence lifetimes, while for the cooler models angular momentum is lost from the surface

Burkhardt C., Coupry M.F., 1989, A&A 220, 197
 Burkhardt C., Coupry M.F., 1991, A&A 249, 205
 Burkhardt C., Coupry M.F., 1998, A&A 338, 1073
 Burkhardt C., Coupry M.F., 1999, A&A, in preparation
 Caughlan G.R., Fowler W.A., 1988, Atomic Data Nuc. Data Tables 40,283
 Chaboyer B., Demarque P., Pinsonneault M.H., 1995, ApJ 441, 865
 Charbonneau P., Michaud G., 1988, ApJ 334, 746
 Charbonneau P., Michaud G., 1990, ApJ 352, 681
 Charbonneau P., Michaud G., 1991, ApJ 370, 693
 Charbonnel C., 1995, ApJ Letters 453, L41
 Charbonnel C., Vauclair S., Zahn J.P., 1992, A&A 255, 191
 Charbonnel C., Vauclair S., 1992, A&A 265, 55
 Charbonnel C., Vauclair S., Maeder A., Meynet G., Schaller G., 1994, A&A 283, 155
 Christensen-Dalsgaard J., Däppen W., et al., 1996, Sci 272, 1286
 Deliyannis C.P., Pinsonneault M.H., 1990, ApJ 365, L67
 Deliyannis C.P., King J.R., Boesgaard A.M., 1997, in "Wide-Field Spectroscopy", Eds.E.Kontizas et al., p.201

Table 2. Logarithm of the dilution factors. The observed values for Li in different open clusters with the quoted turnoff mass are from Gilroy (1989), while the values for field stars are from Lèbre et al. (1999). Be and B observed values are from Duncan et al. (1998)

M_*/M_\odot	V ($\text{km}\cdot\text{sec}^{-1}$)	${}^7\text{Li}$	${}^9\text{Be}$ Predicted	${}^{10}\text{B}$
1.5	150	2.87	1.99	1.11
	100	2.33	1.68	0.98
	50	1.89	1.41	0.84
	0	1.24	0.93	0.46
1.85	150	2.75	1.94	1.11
	100	2.27	1.68	0.99
	50	1.88	1.45	0.87
	0	1.65	1.28	0.76
2.2	150	2.85	1.97	1.15
	100	2.34	1.70	1.04
	50	1.92	1.48	0.90
	0	1.54	1.21	0.70
$M(\text{turnoff})/M_\odot$	Open cluster	${}^7\text{Li}$	${}^9\text{Be}$ Observed	${}^{10}\text{B}$
1.6	NGC 752	1.9 - 3.2		
2.2	Hyades	2 - 2.4	> 1.44	0.7 - 1.3
2.2	Praesepe	2.3 - 2.7		
2.2	IC 4756	2.2 - 3.3		
2.5	NGC 6633	2.3 - 2.9		
2.6	NGC 2548	2.3 - 2.6		
2.7	NGC 2281	3.1 - 3.2		
2.8	Stock 2	2.5 - 3		
2.8	NGC 1545	> 3		
1.5 - 3	Field	2.1 - > 3		

Dias J.D., Charbonnel C., Lèbre A., de Laverny P., De Medeiros J.R., 1999, A&A submitted
 Duncan D.K., Peterson R.C., Thorburn J.A., Pinsonneault M.H., 1998, ApJ 499, 871
 Friel E.D., Boesgaard A.M., 1990 ApJ 351, 480
 Gaigé Y., 1993, A&A 269, 267
 García López R.J., Spruit H.C., 1991, ApJ 377, 268
 García López R.J., Rebolo R., Herrero A., Beckman J.E., 1993, ApJ 412, 173
 Gilroy K.K., 1989, ApJ 347, 835
 Grevesse N., Noels A., 1993, in "Origin and Evolution of the Elements", Eds. Prantzos N., Vangioni-Flam E., Cassé M.
 Guzik J.A., Willson L.A., Brunish W.M., 1987, ApJ 319, 957
 Hobbs L.M., Iben I., Pilachowski C., 1989, ApJ 347, 817
 Iglesias C.A., Rogers F.J., 1996, ApJ 464, 943
 Kraft R.P., 1965, ApJ 142, 681
 Lèbre A., de Laverny P., de Medeiros J.R., Charbonnel C., da Silva L., 1999, A&A 345, 936
 Maeder A., 1983, A&A 120, 113
 Maeder A., 1995, A&A 299, 84
 Mermillod J.C., 1992, private communication
 Michaud G., 1970, ApJ 160, 641
 Michaud G., 1986, ApJ 302, 650

- Michaud G., Charland Y., Vauclair S., Vauclair G., 1976, ApJ 210, 447
- Michaud G., Charbonneau P., 1991, Space Sci. Rev., 57, 1
- Montalban J., Schatzman E., 1994, A&A 305, 513
- Paquette C., Pelletier C., Fontaine G., Michaud G., 1986, ApJS 61, 177
- Pilachowski C.A., Saha A., Hobbs L.M., 1988, PASP 100, 474
- Pinsonneault M.H., Kawaler S.D., Sofia S., Demarque P., 1989, ApJ 338, 424
- Pinsonneault M.H., Kawaler S.D., Demarque P., 1990, ApJS 74, 501
- Proffitt C.R., Michaud G., 1989, ApJ 346, 976
- Richard O., Vauclair S., Charbonnel C., Dziembowski W.A., 1996, A&A 312, 1000
- Richer J., Michaud G., 1993, ApJ 416, 312
- Richer J., Michaud G., Massacrier G., 1997, A&A 317, 968
- Richer J., Michaud G., Turcotte S., 1999a, ApJ, submitted
- Richer J., Michaud G., Talon, S. 1999b, ApJ, in preparation
- Schramm D.N., Steigman G., Dearborn D.S.P., 1990, ApJ 359, L55
- Stauffer J.R., Hartmann L.W., Latham D.W., 1987, ApJ 320, L51
- Swenson F.J., Faulkner J., 1992, ApJ 395, 654
- Talon S., Charbonnel C., 1998, A&A
- Talon S., Zahn J.P., 1997, A&A 317, 749
- Talon S., Zahn J.P., Maeder A., Meynet G., 1997, A&A 322, 209
- Thorburn J., Hobbs L.H., Deliyannis C.P., Pinsonneault M.H., 1993, ApJ 415, 150
- Turcotte S., Richer J., Michaud G., 1998, ApJ 504, 559
- Vauclair G., Vauclair S., Michaud G., 1978, ApJ 223, 920
- Vauclair S., 1988, ApJ 335, 971
- Vauclair S., 1991, Evolution of Stars : The Photospheric Abundance Connection, IAU Symp. 145 (eds G.Michaud & A.Tutukov), 327
- Wallerstein G., Herbig G.H., Conti P.S., 1965, ApJ 141, 610
- Zahn J.-P., 1992, A&A 265, 115